

**Figure 1.** Transition state models for 1,2-induction.

(no regioisomers were detected in any reactions) and follow expected trends for additions of electrophilic radicals.<sup>9</sup> Stereoselectivities in additions to cyclic alkenes also follow established trends: five-membered rings give high trans selectivity (single isomer, entry i), and six-membered rings give modest trans selectivity (70/30, entry j).<sup>10</sup> For acyclic alkenes, addition to styrene **2k** gives modest syn selectivity (80/20, entry k) while addition to *N*-aryl enamine **2n** gives good syn selectivity (90/10, entry n).<sup>11</sup> In contrast, addition to enol ether **2l** gives modest anti selectivity (25/75, entry l), and addition to phenylthio enol ether **2m** gives good anti selectivity (10/90, entry m).<sup>11</sup>

All documented examples of 1,2-induction in radical reactions (including those above) involve conjugated radicals. To probe the reactions of alkyl radicals, we conducted iodine transfer reactions of **4** with a short series of disubstituted alkenes (**2o–q**), and the results are summarized in eq 2. There was no selectivity in the addition of **4** to **2o**, modest syn selectivity in the addition to **2p** (75/25), and very high syn selectivity in the addition to **2q** (98/2).<sup>11</sup> This level of selectivity is impressive, especially considering that iodine transfer from an iodomalnonitrile to an alkyl radical is an extremely rapid reaction.<sup>12</sup>

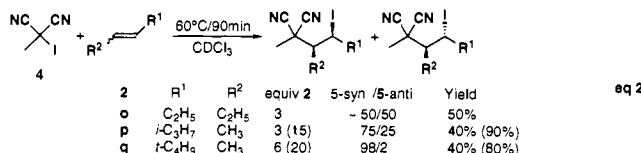


Figure 1 shows models for each of the 1,2-induction reactions. At this early stage, we consider only the size effects of the malononitrile group; further experiments will be needed to identify any electronic or stereoelectronic contributions. The large majority of existing examples of 1,2-induction follow an A-strain model (Figure 1a);<sup>2,4</sup> a conjugating substituent on the radical-bearing carbon dictates that the smallest substituent on the adjacent stereocenter (hydrogen) occupies the “inside” position. The medium group is “outside”, and the large group is “anti”. Selenium-, iodine-,<sup>4b</sup> and deuterium-transfer<sup>4b</sup> reactions of the benzylic radical derived from  $\beta$ -methylstyrene all follow this model (Figure 1a) and give similar syn selectivities (80/20 to 85/15). We and Giese have recently shown that oxygen-substituted radicals do not follow the A-strain model and, instead, follow a “Felkin–Anh” model;<sup>3</sup> the medium-sized group is inside, and the hydrogen is outside (Figure 1b). Addition of **1** of **2l** is indeed in line with this

(9) (a) Giese, B. *Angew. Chem., Int. Ed. Engl.* **1983**, *22*, 753. (b) Giese, B.; Horler, H.; Leising, M. *Chem. Ber.* **1986**, *119*, 444. (c) Renaud, P.; Schubert, S. *Synlett* **1991**, 624. (d) Renaud, P.; Vionnet, J. P.; Vogel, P. *Tetrahedron Lett.* **1991**, *32*, 3491.

(10) Giese, B. *Angew. Chem., Int. Ed. Engl.* **1989**, *28*, 969.

(11) Full details of configurational assignments are provided in the supplementary material.

(12) See ref 5b and the following: Curran, D. P.; Bosch, E.; Kaplan, J.; Newcomb, M. *J. Org. Chem.* **1989**, *54*, 1826.

radical version of the Felkin–Anh model. The sulfur-substituted radical derived from addition of **1** to **2m** gives even higher “Felkin–Anh” selectivity than its oxygen counterpart. Geometric parallels<sup>1</sup> between enamines,<sup>13a</sup> iminium ions, and nitrogen-substituted radicals suggest that the nitrogen-substituted radicals should follow the A-strain model rather than the Felkin–Anh model (Figure 1c); again the results agree (entry m). Finally, the series of additions in eq 2 shows for the first time that conjugation is not indispensable. If the substituent on the radical center becomes large enough, then excellent syn selectivity can be expected (see **5q**). For this reaction, we tentatively suggest the model in Figure 1d. We suspect that conformations of these types of radicals (and ultimately of the transition states) are restricted by the need for the large group on the radical to be distant from both the medium and large groups on the adjacent stereocenter.

Even though selenium transfer<sup>7</sup> must be slower than iodine transfer, the replacement of iodine by phenylselenium significantly extends the scope of malononitrile radical chemistry by permitting additions to classes of alkenes that are not well-behaved in additions of iodomalnonitriles. The additions of selenomalnonitrile **1** have already opened new directions in 1,2-asymmetric induction, and further new preparative directions should be revealed by the union of these radical reactions with organoselenium-based methods in organic synthesis.

**Acknowledgment.** We thank the National Institutes of Health for funding and for a Research Career Development Award (to D.P.C.). D.P.C. thanks the Dreyfus Foundation for a Teacher Scholar Award, and G.T. thanks the Deutsche Forschungsgemeinschaft for a postdoctoral fellowship. We are especially grateful to Dr. Steven Geib for solving the crystal structure of **5q**-syn.

**Supplementary Material Available:** Procedures for the synthesis of **1** and **4**, characterization and structure assignments for all products of 1,2-induction reactions, and complete details of the X-ray crystal structure of **5q**-syn (11 pages). Ordering information is given on any current masthead page.

(13) (a) Hoffmann, R. W. *Chem. Rev.* **1989**, *89*, 1841. (b) Nagai, M.; Gaudino, J. J.; Wilcox, C. S. *Synthesis* **1992**, 163.

## Mechanism of Rhodium(III)-Catalyzed Methyl Acrylate Dimerization

Maurice Brookhart\* and Elisabeth Hauptman

Department of Chemistry  
University of North Carolina  
Chapel Hill, North Carolina 27599-3290  
Received January 22, 1992

Recently we reported a highly efficient Rh-based catalytic system<sup>1</sup> for the selective tail-to-tail dimerization of methyl acrylate (MA) to dimethyl hexenedioates, precursors to adipic acid, which is an intermediate in nylon-66 production.<sup>1–3</sup> The catalytic cycle is entered by protonation of Cp\*Rh(C<sub>2</sub>H<sub>4</sub>)<sub>2</sub>, **1**, in the presence of MA.<sup>4</sup> The catalyst is deactivated by loss of H<sub>2</sub> to give the

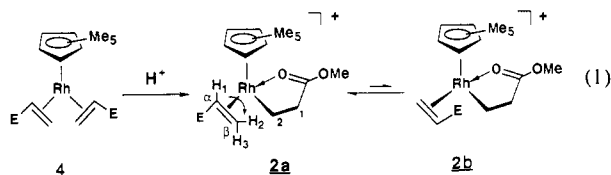
(1) Brookhart, M.; Sabo-Etienne, S. *J. Am. Chem. Soc.* **1991**, *113*, 2777.

(2) For reports of other Rh-based acrylate dimerization catalysts, see: (a) Alderson, T. U.S. Patent 3013066, 1961. (b) Alderson, T.; Jenner, E. L.; Lindsey, R. V. *J. Am. Chem. Soc.* **1965**, *87*, 5638. (c) Nugent, W. A.; McKinney, R. J. *J. Mol. Catal.* **1985**, *29*, 65. (d) Singleton, D. M. U.S. Patent 4638084, 1987. For related vinyl ketone dimerization, see: (e) Kovalev, I. P.; Kolmogorov, Y. N.; Strelenko, Y. A.; Ignatenko, A. V.; Vinogradov, M. G.; Nikishin, G. I. *J. Organomet. Chem.* **1991**, *420*, 125. (f) Nikishin, G. I.; Kovalev, I. P.; Klimova, T. E.; Ignatenko, A. V. *Tetrahedron Lett.* **1991**, *32*, 1077.

(3) For references to Pd-, Ni-, and Ru-based acrylate dimerization catalysts, see footnotes 4 and 5 of ref 1.

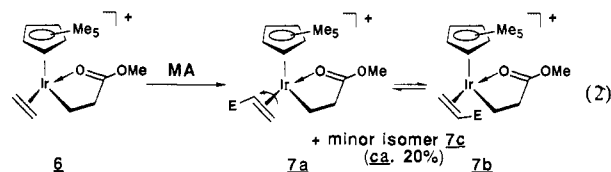
$\pi$ -allyl complex  $\text{Cp}^*\text{Rh}(\eta^3\text{-MeOC(O)CH}_2\text{CHCHCO}_2\text{Me})^+$ , **3**. Exposure of **3**, obtained together with dimers and remaining MA, to  $\text{H}_2$  results in catalyst regeneration. Alternatively, a long-lived catalyst system can be operated under 1 atm of  $\text{H}_2$ . While a  $^1\text{H}$  signal at  $\delta$  1.6 for the  $\text{Cp}^*$  ligand of the catalyst resting state could be observed,<sup>1</sup> the structure of this species, the mode of C-C bond coupling, and details of the catalytic cycle were unknown. We report here low-temperature spectroscopic characterization of the resting state and observation of the carbon-carbon coupling process which demonstrate the key mechanistic features of the catalytic cycle. Results using iridium analogs are also described which offer supporting evidence for the structure of the catalyst resting state.

Treatment of **1** with methyl acrylate at 130 °C for 4 h results in formation of  $\text{Cp}^*\text{Rh}(\text{CH}_2=\text{CHCO}_2\text{Me})_2$  as a mixture of isomers (ca. 90% yield). After successive recrystallizations, one pure isomer, **4**, can be isolated.<sup>5</sup> Protonation of **4** in  $\text{CD}_2\text{Cl}_2$  at -78 °C leads to the formation of **2** (eq 1). The  $^1\text{H}$  resonance



of the  $\text{Cp}^*$  ligand appears at 1.6 ppm, which corresponds to the shift observed for the resting state during bulk dimerization.<sup>1</sup> Presence of an  $\eta^2$ -methyl acrylate is confirmed by a typical  $^1\text{H}$  pattern for the olefinic protons (4.67 ppm, dd,  $J_{\text{trans}} = 13$  Hz,  $J_{\text{cis}} = 9$  Hz,  $\text{H}_1$ ; 3.95 ppm, d,  $J_{\text{trans}} = 13$  Hz,  $\text{H}_3$ ; 3.30 ppm, d,  $J_{\text{cis}} = 9$  Hz,  $\text{H}_2$ ) and  $^{13}\text{C}$  signals at 72.9 ppm (dd,  $J_{\text{C-Rh}} = 8$  Hz,  $J_{\text{C-H}} = 164$  Hz,  $\text{C}_\alpha$ ) and 69.0 ppm (dt,  $J_{\text{C-Rh}} = 10$  Hz,  $J_{\text{C-H}} = 164$  Hz,  $\text{C}_\beta$ ). The chelate structure is verified by  $^{13}\text{C}$  signals at 22.2 ppm (dt,  $J_{\text{C-Rh}} = 18$  Hz,  $J_{\text{C-H}} = 150$  Hz) for  $\text{C}_2$  and 39.6 (t,  $J_{\text{C-H}} = 127$  Hz) for  $\text{C}_1$ . The spectroscopic data, however, do not indicate the relative orientation of the  $\eta^2$ -olefin and the chelate.

Seeking additional information regarding the structure of the resting state, **2**, the iridium analogs were investigated. Protonation of  $\text{Cp}^*\text{Ir}(\text{C}_2\text{H}_4)_2$ ,<sup>6</sup> **5** ( $\text{CH}_2\text{Cl}_2$ , 25 °C), in the presence of methyl acrylate leads sequentially to **6**<sup>5</sup> and then **7**<sup>5</sup> (eq 2). Complex **6** is fluxional;  $^1\text{H}$  and  $^{13}\text{C}$  NMR spectroscopy indicate that the dynamic process is ethylene rotation.<sup>5</sup> Complex **7** consists of a mixture of two major isomers **7a,b** (80%, 1:1 ratio) and one minor isomer **7c** (ca. 20%) detected spectroscopically at -78 °C.<sup>5</sup>



Variable-temperature  $^1\text{H}$  and  $^{13}\text{C}$  NMR spectra show that the two major isomers undergo rapid interconversion via  $\eta^2$ -acrylate rotation ( $k = 132$  s<sup>-1</sup>,  $\Delta G^\ddagger = 14.3$  kcal/mol, 20 °C). Crystallization of **7** from diethyl ether/hexane gives light yellow plates, which were shown to be **7a** by single-crystal X-ray analysis.<sup>7</sup> Isomer **7a** is one of the major isomers since dissolution of the plates

(4) The acid used for all protonations was  $\text{HB}(\text{C}_6\text{H}_3(\text{CF}_3)_2)_4(\text{Et}_2\text{O})_2$ . The counterion increases the solubilities of intermediate salts: Kobayashi, H.; Nishida, H.; Takada, N.; Yoshimura, M.; Sonoda, T. *Bull. Chem. Soc. Jpn.* **1984**, *57*, 2600.

(5) See supplementary material for synthesis and complete spectroscopic characterization.

(6)  $\text{Cp}^*\text{Ir}(\text{C}_2\text{H}_4)_2$  was prepared according to a reported procedure: Maitlis, P. M.; Moseley, K.; Kang, J. W. *J. Chem. Soc. A* **1970**, 2875. For an improved procedure for the preparation of  $(\text{Cp}^*\text{IrCl}_2)_2$ , see: Heinekey, D. M.; Ball, R. G.; Graham, W. A. G.; Hoyano, J. K.; McMaster, A. D.; Mattson, B. M.; Michel, S. T. *Inorg. Chem.* **1990**, *29*, 2023.

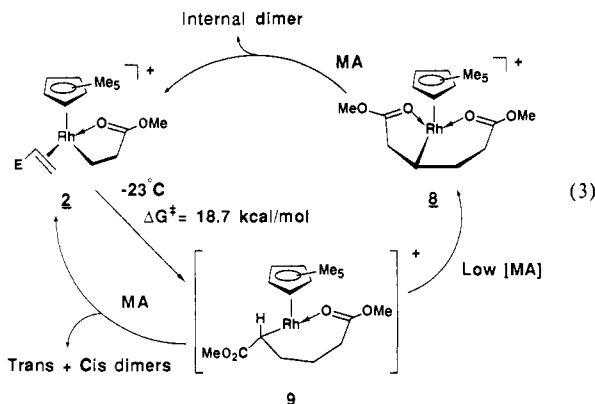
(7) The X-ray diffraction study was carried out by J. C. Calabrese at E. I. du Pont de Nemours & Co., Inc., Experimental Station, P.O. Box 80328, Wilmington, DE. See supplementary material for a summary of the crystal data and an ORTEP diagram of **7a**.

in  $\text{CD}_2\text{Cl}_2$  at -78 °C gives only the rapidly equilibrating pair (**7a**, **7b**); upon warming to 23 °C the minor isomer **7c** grows in. The orientation of the acrylate ligands observed in **7a** is that required for tail-to-tail coupling. Thus, this complex is a model for the structure of the rhodium complex just prior to C-C coupling and is likely isostructural with the resting state **2**.

Although the iridium system is a good structural model for the resting state **2**, its lack of reactivity prevents further mechanistic study. In contrast, significant mechanistic information results from warming the rhodium resting state **2** in the absence of monomer and monitoring it spectroscopically. Complex **2** is fluxional since its  $^1\text{H}$  signals broaden at temperatures above ca. -50 °C, but rearrangement of **2** occurs before coalescence can be reached. On the basis of the iridium system, this fluxional behavior presumably reflects interconversion of major and minor isomers **2a,b** via  $\eta^2$ -methyl acrylate rotation. We assign the major isomer as **2a** (with proper alignment for C-C coupling) in analogy with **7a**, but there is no additional data which supports this assignment.

A critical observation is that complex **2** rapidly rearranges to **8** above ca. -50 °C. At -23 °C, the first-order rate constant for isomerization is  $2.4 \times 10^{-4}$  s<sup>-1</sup>,  $\Delta G^\ddagger = 18.7$  kcal/mol. This free energy of activation is the same as the one obtained earlier from the turnover (TO) frequency in the catalytic system: 6.6 TO/min at 25 °C,  $\Delta G^\ddagger = 19$  kcal/mol. The correspondence of these barriers lends support to the identity of the resting-state structure as **2** and the assignment of the turnover-limiting step in the cycle as  $\text{C}_2\text{-C}_\beta$  coupling.

The isomerization of **2** to **8** must proceed by migration of the  $\sigma$ -bound carbon of the chelate to  $\text{C}_\beta$  of the  $\eta^2$ -acrylate. Initially this migratory insertion process results in **9**,<sup>8</sup> which can form **8** by a  $\beta$ -hydride elimination/readdition sequence (eq 3). It is instructive to note that the  $\Delta G^\ddagger$  for this migratory insertion (**2**  $\rightarrow$  **9**) is reasonably close to the  $\Delta G^\ddagger$  of 22.3 kcal/mol for migratory insertion in the simple model system  $\text{Cp}^*(\text{P}(\text{OMe})_3)\text{Rh}(\text{CH}_2=\text{CH}_2)(\text{CH}_2\text{CH}_3)^+$  we examined previously.<sup>9</sup>



Treatment of **8** with MA at -20 °C results in displacement of dimer and regeneration of the resting state **2**. Careful monitoring of the dimers formed from **8** and **2** at low turnover numbers suggests that **8** is not an intermediate in the major catalytic cycle. Treatment of **2** with MA (60 equiv) gives *only trans-* and *cis-*  $\text{MeO}_2\text{CCH}=\text{CHCH}_2\text{CH}_2\text{CO}_2\text{Me}$  after 6 turnovers. However, reaction of **8** with MA (25 equiv) yields 40% internal isomer *trans*- $\text{MeO}_2\text{CCH}_2\text{CH}=\text{CHCH}_2\text{CO}_2\text{Me}$  after ca. 3 turnovers, suggesting that **8** releases nearly exclusively internal isomer.<sup>10</sup> The major catalytic cycle must thus involve interception of **9** (or a similar intermediate<sup>8</sup>) by MA to return to **2** (see eq 3). Only at very low MA concentrations does formation of **8** from **9** compete with direct regeneration of **2**. Preliminary results suggest that the inactive  $\pi$ -allyl complex **3** forms by transfer of  $\text{H}_2$  from **8** to

(8) An 18-electron configuration for **9** could be achieved through  $\pi$ -interaction with the carbonyl group resulting in an oxoallyl structure.

(9) Brookhart, M.; Lincoln, D. M. *J. Am. Chem. Soc.* **1988**, *110*, 8719.

(10) Once the dimerization is complete, metal-catalyzed isomerization of the dimers occurs to give the *trans/cis/internal* isomers in a ca. 90:5:5 ratio.

either MA or dimer to give, respectively, methyl propionate or dimethyl adipate.

**Acknowledgment.** We thank J. C. Calabrese (Du Pont) for the X-ray structural analysis and P. J. Fagan (Du Pont) for helpful discussions. This work was supported by the National Science Foundation (CHE-8705534) and by E. I. du Pont de Nemours & Co., Inc. We also thank Johnson Matthey for a loan of  $\text{RhCl}_3$ .

**Supplementary Material Available:** A listing of the synthetic procedures used to prepare **2**, **4**, **6**, and **7**,  $^1\text{H}$  and  $^{13}\text{C}$  NMR spectral data for **2**, **4**, **6**, and **7**, microanalytical data for **4**, **6**, and **7**, details of kinetic calculations, and crystal data and an ORTEP diagram for **7a** (9 pages). Ordering information is given on any current masthead page.

### Stereochemistry of Chiral, Nonracemic Lithium Salts of Acyclic $\alpha$ -Sulfonyl Carbanions: The Asymmetric Induction Exerted by the Lithium-Coordinated Sulfonyl Group

Hans-Joachim Gais\* and Gunther Hellmann

Institut für Organische Chemie der  
Rheinisch-Westfälischen Technischen Hochschule Aachen  
Prof.-Pirlet-Strasse 1, D-5100 Aachen, Germany

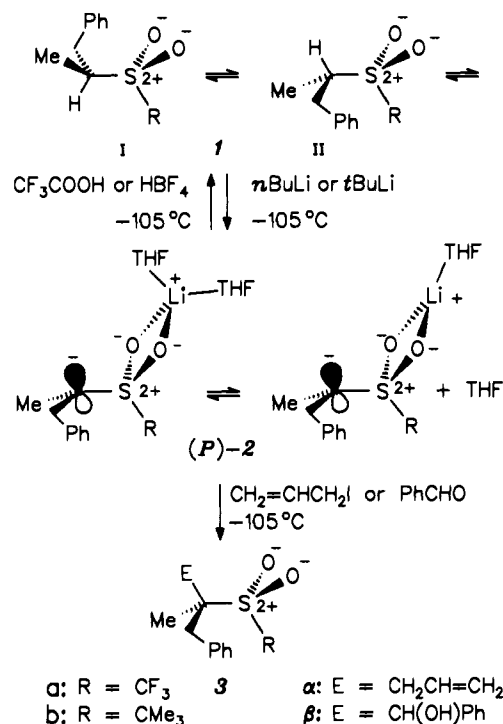
Received January 21, 1992

We have recently described the synthesis of the lithio (tri-fluoromethyl)sulfone (*M*)-(-)-**2a**<sup>1,2</sup> (Scheme I), which has an extrapolated half-life for racemization of 30 days at  $-78^\circ\text{C}$ . It belongs to the exceedingly small group<sup>3</sup> of functionalized chiral, nonracemic organolithium compounds which are configurationally stable on a synthetic time scale while lacking elements of auxiliary chirality. The attainment of (*M*)- and (*P*)-**2a**<sup>1,2,4</sup> allowed for the first time the study of the asymmetric induction exerted by the sulfonyl group at the  $\alpha$ -C atom in lithium salts of acyclic  $\alpha$ -sulfonyl carbanions. The stereochemistry of deuteration and protonation of transient chiral, nonracemic acyclic  $\alpha$ -sulfonyl carbanions has been studied through base-catalyzed H/D-exchange, retro-aldol, and decarboxylation reactions of optically active sulfones.<sup>5</sup>

We report herein on the synthesis and racemization kinetics of a new chiral, nonracemic lithio sulfone, the lithio *tert*-butylsulfone (*P*)-(+)-**2b** (Scheme I), and on the stereochemistry of the formation and protonation as well as alkylation of (*P*)-(+)-**2a** and (*P*)-(+)-**2b**.

(*P*)-**2b** was generated by deprotonation of the sulfone (*S*)-**1b**<sup>4</sup> ( $\geq 99\%$  ee<sup>6a</sup>) in THF at  $-105^\circ\text{C}$  with *n*-BuLi in THF<sup>7</sup> and its

Scheme I



racemization in the presence of DMPU (4 equiv)<sup>8</sup> monitored polarimetrically at low temperatures as a function of time.<sup>4</sup> The process was found to follow pseudo-first-order kinetics. This allowed for a determination of the activation parameters  $\Delta G^\ddagger_{298} = 13.0 \pm 0.3 \text{ kcal mol}^{-1}$ ,  $\Delta H^\ddagger = 13.2 \pm 0.3 \text{ kcal mol}^{-1}$ , and  $\Delta S^\ddagger = 0.6 \pm 1.2 \text{ cal mol}^{-1} \text{ K}^{-1}$ , which translate into an extrapolated half-life of 3 h at  $-105^\circ\text{C}$ . A comparison with the activation parameters  $\Delta G^\ddagger_{298} = 17.3 \pm 0.3 \text{ kcal mol}^{-1}$ ,  $\Delta H^\ddagger = 16.7 \pm 0.3 \text{ kcal mol}^{-1}$ , and  $\Delta S^\ddagger = -1.9 \pm 1.1 \text{ cal mol}^{-1} \text{ K}^{-1}$  for the racemization of (*M*)-**2a** in THF<sup>1</sup> reveals, besides a very small entropic contribution in both cases, a lower barrier to  $\text{C}\alpha$ -S bond rotation in (*P*)-**2b**, which we ascribe to a reduced  $n_{\text{C}}-\sigma_{\text{SR}}^*$  hyperconjugation as well as Coulombic interaction.<sup>1,9</sup> Restricted  $\text{C}\alpha$ -S bond rotation due to torsional as well as electronic effects, not restricted inversion of the  $\alpha$ -C atom, is decisive for the configurational stability of (*P*)-**2b**. This follows, among other conclusions, from the similar activation parameters obtained by  $^1\text{H}$  DNMR spectroscopy for the enantiomerization of ( $\pm$ )-lithium 1-(*tert*-butylsulfonyl)-1,2-diphenylethane,<sup>9</sup> whose  $\alpha$ -C atom is planar,<sup>4</sup> and of *rac*-**2b**,<sup>4</sup> whose  $\alpha$ -C atom is most probably pyramidal.<sup>10</sup>

Deprotonation of the sulfones (*S*)-**1a**<sup>1,4</sup> ( $\geq 98\%$  ee<sup>6b</sup>) and (*S*)-**1b**<sup>4</sup> ( $\geq 99\%$  ee<sup>6a</sup>) in THF at  $-105^\circ\text{C}$  with *n*-BuLi (1 equiv) in *n*-hexane or THF<sup>7</sup> (3 min<sup>11</sup>) led to the lithio sulfones (*P*)-**2a** and (*P*)-**2b**, respectively. They gave, upon protonation at  $-105^\circ\text{C}$  with  $\text{CF}_3\text{COOH}$  (4 equiv) in THF,<sup>7</sup> with overall retention of configuration, (*S*)-**1a** (97%) of 82% ee<sup>6c</sup> and (*S*)-**1b** (98%) of 90% ee,<sup>6a,c</sup>

(1) Gais, H.-J.; Hellmann, G.; Günther, H.; Lopez, F.; Lindner, H. J.; Braun, S. *Angew. Chem.* **1989**, *101*, 1061; *Angew. Chem., Int. Ed. Engl.* **1989**, *28*, 1025.

(2) For the descriptors *M* and *P*, see: Prelog, V.; Helmchen, G. *Angew. Chem.* **1982**, *94*, 614; *Angew. Chem., Int. Ed. Engl.* **1982**, *21*, 567.

(3) (1-Isocyanato-2,2-diphenylcyclopropyl)lithium: Periasamy, M. P.; Walborsky, H. M. *J. Am. Chem. Soc.* **1977**, *99*, 2631. ( $\alpha$ -Alkoxyalkyl)lithium compounds: Still, W. C.; Sreekumar, C. *J. Am. Chem. Soc.* **1980**, *102*, 1201. McGarvey, G. J.; Kimura, M. *J. Org. Chem.* **1982**, *47*, 5420. Hoppe, D.; Krämer, T. *Angew. Chem.* **1986**, *98*, 171; *Angew. Chem., Int. Ed. Engl.* **1986**, *25*, 160. Chan, P. C.-M.; Chong, J. M. *J. Org. Chem.* **1988**, *53*, 5586. Matteson, D. S.; Tripathy, P. B.; Sarkar, A.; Sadhu, K. M. *J. Am. Chem. Soc.* **1989**, *111*, 4399. Marshall, J. A.; Gung, W. Y. *Tetrahedron* **1989**, *45*, 1043. Chong, J. M.; Mar, E. K. *Tetrahedron* **1989**, *45*, 7709. Zschage, O.; Schwark, J.-R.; Hoppe, D. *Angew. Chem.* **1990**, *102*, 336; *Angew. Chem., Int. Ed. Engl.* **1990**, *29*, 296. Hoppe, D.; Carstens, A.; Krämer, T. *Angew. Chem.* **1990**, *102*, 1455; *Angew. Chem., Int. Ed. Engl.* **1990**, *29*, 1424.

(4) Hellmann, G. Ph.D. Thesis, Universität Freiburg, 1991.

(5) Cram, D. J.; Nielsen, W. D.; Rickborn, B. *J. Am. Chem. Soc.* **1960**, *82*, 6415. Corey, E. J.; Kaiser, E. T. *J. Am. Chem. Soc.* **1961**, *83*, 490. Cram, D. J.; Scott, D. A.; Nielsen, W. D. *J. Am. Chem. Soc.* **1961**, *83*, 3696. Corey, E. J.; König, H.; Lowry, T. H. *Tetrahedron Lett.* **1962**, 515. Cram, D. J.; Wingrove, A. S. *J. Am. Chem. Soc.* **1963**, *85*, 1100. Corey, E. J.; Lowry, T. H. *Tetrahedron Lett.* **1965**, 793. Corey, E. J.; Lowry, T. H. *Tetrahedron Lett.* **1965**, 803. Cram, D. J.; Trepka, R. D.; Janiak, P. S. *J. Am. Chem. Soc.* **1966**, *88*, 2749.

(6) Analysis was by (a) 400-MHz  $^1\text{H}$  NMR spectroscopy ( $\text{CDCl}_3$ ) with  $\text{Eu}(\text{hfc})_3$ , (b) 400-MHz  $^1\text{H}$  NMR spectroscopy ( $\text{CDCl}_3$ ) of the precursor of (*S*)-**1a**, (*S,R/S*)- $\text{PhCH}_2\text{CH}(\text{CH}_3)\text{S}(\text{O})\text{CF}_3$ ,<sup>1,4</sup> with  $\text{Eu}(\text{hfc})_3$ , (c) optical rotation, and (d) 400-MHz  $^1\text{H}$  NMR spectroscopy ( $\text{CDCl}_3$ ) with  $\text{Ag}(\text{fod})$  and  $\text{Pr}(\text{tfc})_3$ .

(7) The solution was precooled to about  $-80^\circ\text{C}$ .

(8) Racemization of (*P*)-**2a** and (*P*)-**2b** in THF is slower in the presence of *N,N'*-dimethyl-*N,N'*-propyleneurea (DMPU) (Mukhopadhyay, T.; Seebach, D. *Helv. Chim. Acta* **1982**, *65*, 385 and references cited therein), thereby allowing in the latter case for a determination of the temperature dependency of  $k_{\text{rac}}$  at experimentally more convenient temperatures.<sup>1,4</sup>

(9) Gais, H.-J.; Hellmann, G.; Lindner, H. *Angew. Chem.* **1990**, *102*, 96; *Angew. Chem., Int. Ed. Engl.* **1990**, *29*, 100.

(10) (a) Gais, H.-J.; Vollhardt, J.; Hellmann, G.; Paulus, H.; Lindner, H. *J. Tetrahedron Lett.* **1988**, *29*, 1259. (b) Gais, H.-J.; Müller, J.; Vollhardt, J.; Lindner, H. *J. Am. Chem. Soc.* **1991**, *113*, 4002.

(11) Quantitative deprotonation of (*S*)-**1a** and (*S*)-**1b** after the time given was ascertained in each case by deuteration.